Aero-Thermal Calibration of the NASA Glenn Icing Research Tunnel (2012 Test)

Christine M. Pastor-Barsi,* E. Allen Arrington, †
and Judith Foss Van Zante‡
Sierra Lobo, Inc. at NASA Glenn, Cleveland, OH, 44135

A major modification of the refrigeration plant and heat exchanger at the NASA Glenn Icing Research Tunnel (IRT) occurred in autumn of 2011. It is standard practice at NASA Glenn to perform a full aero-thermal calibration of the test section of a wind tunnel facility upon completion of major modifications. This paper will discuss the tools and techniques used to complete an aero-thermal calibration of the IRT and the results that were acquired.

The goal of this test entry was to complete a flow quality survey and aero-thermal calibration measurements in the test section of the IRT. Test hardware that was used includes the 2D Resistive Temperature Detector (RTD) array, 9-ft pressure survey rake, hot wire survey rake, and the quick check survey rake. This test hardware provides a map of the velocity, Mach number, total and static pressure, total temperature, flow angle and turbulence intensity. The data acquired were then reduced to examine pressure, temperature, velocity, flow angle, and turbulence intensity. Reduced data has been evaluated to assess how the facility meets flow quality goals. No icing conditions were tested as part of the aero-thermal calibration. However, the effects of the spray bar air injections on the flow quality and aero-thermal calibration measurements were examined as part of this calibration.

Nomenclature

Symbols

A	Conductive heat transfer, hot wire/film
B	Convective heat transfer, hot wire/film
C_0, C_1, C_2	RTD probe total temperature flow recovery curve fit coefficients
C_α	Pitch angle pressure coefficient
C_β	Yaw angle pressure coefficient
C_o	Total pressure coefficient (9-foot rake pressure probes)
C_q	Static pressure coefficient (9-foot rake pressure probes)
E	hot wire anemometer output voltage, volts
$K_0 to K_2$	Flow angle prediction coefficients, degrees
l	characteristic length, ft
M	Mach number
N	Number of data points
n	coefficient, hot wire/film
P	Pressure, psia
$P_1 to P_9$	Flow angle probe pressures, psia
P_{air}	Spray bar air pressure, psig
P_{avg}	Average of P_1, P_2, P_3, and P_4, psia
P_{rat}	Ratio of static to total pressure
P_S	Static pressure, psia (psf)

*AeroMechanical Test Engineer, Test Engineering Services, 21000 Brookpark Road, MS 6-2, AIAA Member.
†Engineering Manager, Test Engineering Services, 21000 Brookpark Road, MS 6-8, AIAA Associate Fellow.
‡AeroMechanical Test Engineer, Test Engineering Services, 21000 Brookpark Road, MS 6-2, AIAA Senior Member.

$P_{S,rake}$	Average of P_6, P_7, P_8, and P_9 (probe static pressure), psia
P_T	Total pressure, psia (psf)
$P_{T,rake}$	Equal to P_5 (probe total pressure), psia
Q	Measured velocity, hot wire/film
q	Dynamic pressure, psi
R	Specific gas constant for air, $1716\frac{ft^2}{(sec^2 \circ R)}$
Re	Reynolds number
T	Temperature, $^\circ C(^\circ F)$
T_s	Static temperature, $^\circ C(^\circ F)$
T_T	Total temperature, $^\circ C(^\circ F)$
$T_{T,davg}$	Average of the 24 D-corner total temperature measurements, $^\circ C(^\circ F)$
$T_{T,dc}$	D-corner total temperature measurement, $^\circ C(^\circ F)$
U	Velocity, knots (ft/sec, mph)
X	Axial coordinate with axis origin at bellmouth/test section weld seam, inches
Y	Spanwise coordinate with axis origin at the test section inner wall, inches
Z	Vertical coordinate with axis origin at the test section floor, inches
α	Pitch flow angle, degrees
β	Yaw flow angle, degrees
γ	Ratio of specific heats, 1.4
Δ	Measured pitch or yaw angle offset, degrees
Subscript	
arm	6-degree of freedom inspection arm
array	2D RTD array
avg	Average
bm	Tunnel bellmouth
i	Data point index
j	Data point index
level	Digital level, inclinometer
local	Test section parameters after all calibration coefficients have been included
rake	9-ft survey rake
ruler	Ruler or tape measure
ts	Tunnel test section

I. Introduction

During January and May 2012, aero-thermal calibration data were acquired at the NASA Glenn Research Center (GRC) Icing Research Tunnel (IRT). Typically full calibrations are completed every five years. The most recent previous full calibration of the IRT was completed in early 2009. The calibration testing performed in 2012 was completed as a result of a major facility upgrade of the refrigeration plant and the heat exchanger. The aero-thermal calibration is one of several tests, including the icing cloud calibration[1], and flow quality surveys in the settling chamber[2], which were performed to re-qualify the IRT after the upgrade. In addition to this work, air flow and liquid water concentration simulations[3] of the IRT were completed by students at the University of Virginia.

The data presented here was acquired using the 9-ft horizontal survey rake, the 2D Resistive Temperature Detector (RTD) array, hot wire vertical survey rake, and the quick check survey rake. The temperature data acquired using the 2D RTD array was used to calibrate the tunnel total temperature probes, which is an array of 24 RTDs located upstream of the test section on the D-corner turning vanes. The static and total pressure data acquired using the 9-ft survey rake were used to calibrate the tunnel north and south pitot-static probes located at the bellmouth of the test section. The data that were acquired using the hot wire rake were used to evaluate turbulence intensity.

Data acquired during the 2012 calibration entry shows that the pressures are consistent with previous calibrations and there has been an improvement on the spatial temperature deviation of the heat exchanger. The temperature profile in the IRT was found to be much more uniform with the new heat exchanger, both at D-corner and the test section, than with the previous heat exchanger.

II. Icing Research Tunnel Description

A schematic of the NASA Glenn Icing Research Tunnel (IRT) is shown in Figure 1. The IRT is a closed loop atmospheric tunnel. The test section is a 6-feet high by 9-feet wide and 20-feet in length. The spraybars which inject atomized water into the flow stream to create the icing conditions are located in the settling chamber between the D-corner turning vanes and the bellmouth inlet.

Operational velocities of the IRT range from 25 knots to 350 knots and tunnel total temperature is controllable from $+20\,°C$ total temperature to $-40\,°C$ test section static temperature. The recently upgraded heat exchanger which enables this range of temperatures is located between C and D corners on the left in Figure 1. Additionally, the upgraded refrigeration plant is located adjacent to the tunnel near the C-corner. Pushing airflow around the circuit is a 5000-horsepower electric motor driving a 25-foot diameter, 12-blade wooden fan[4].

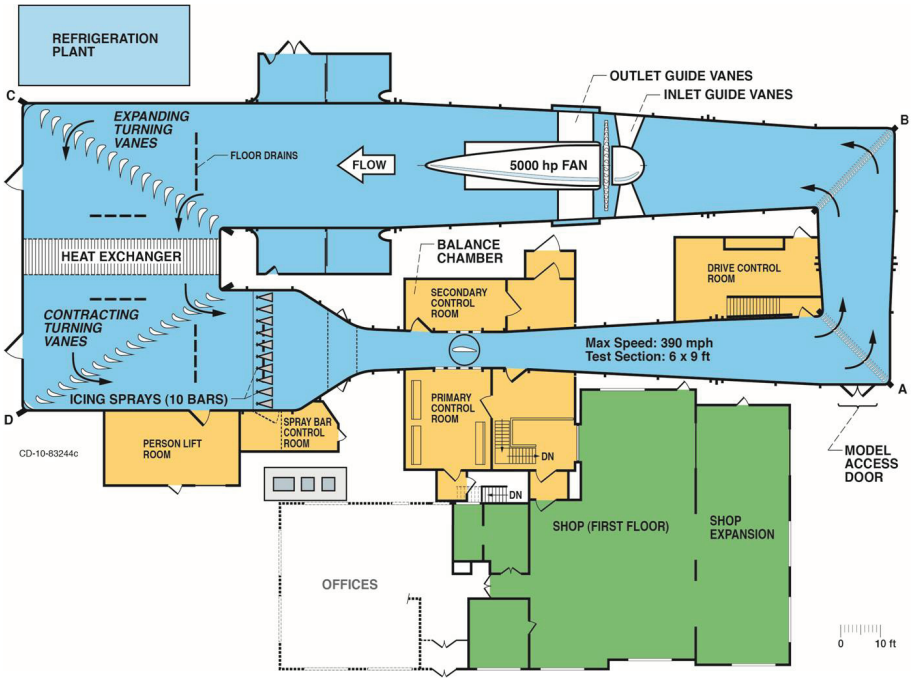

Figure 1. Schematic of the NASA Glenn Icing Research Tunnel

III. Test Hardware and Facility Instrumentation

A. Test Section Resistive Temperature Detector

The 2D Resistive Temperature Detector (RTD) Survey Array is a 7x7 grid of RTDs shown in Figure 2. Probes are spaced at 0%, ±25%, ±50%, and ±75% of the test section both horizontally and vertically. Probes extend 7-inches forward of the leading edge of the 2D RTD array. The leading edge of the probes are positioned 15-inches downstream of the model turn table center. The total temperature probes used in the array are 4-wire RTDs with a ceramic capsule sensor. Total temperature flow recovery testing occurred in 2005[5].

B. 9-foot Survey Rake

The 9-foot survey rake (Figure 3) is used to measure total pressure, static pressure, thereby enabling calculations of velocity and flow angularity. The rake is supported in the center with a vertical strut and at both ends by plates with a bolt pattern which enables positioning of the rake every 6-inches above and below vertical centerline. Additionally, the 9-ft survey rake probes are positioned at the axial position of the center point of the model turn table. Figure 3 illustrates the left handed X-Y-Z coordinate system that is used with the points of origin as follows. The origin for the X-axis is at the bellmouth to test section weld seam.

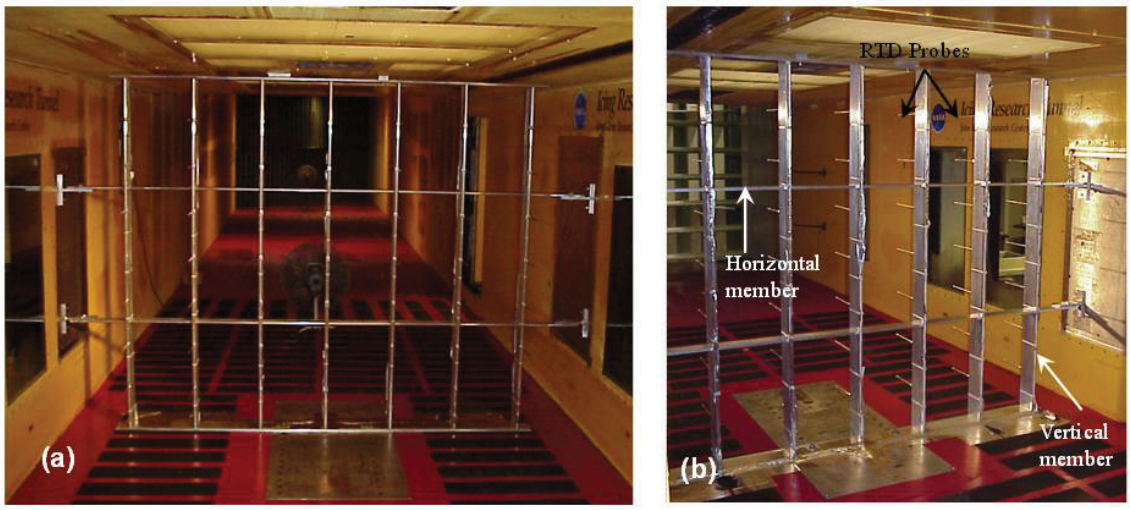

Figure 2. RTD Array installed in the IRT test section. (a) View looking downstream. (b) View looking upstream.

The origin for the Y-axis is the bottom of the inner wall where the wall meets the floor. The origin for the Z-axis is at the floor where the floor meets the inner wall.

The pressure probes, are nominally positioned in 9-inch increments. The hemispherical-head, 5-hole pressure probes (Figure 4) have a single total pressure probe at the center front of the probe to measure total pressure, and 4 additional pressure ports which are in 90 ° increments around the probe head at 45 ° offsets to measure pitch and yaw angle of the airflow. In addition there are 4 static pressure ports 5.75-inches downstream of the head, at 90 ° increments (Figure 4). The probes were all calibrated for Mach 0.1 through 0.6 at the NASA Glenn 3.5-inch diameter free jet calibration facility[6].

Figure 3. The 9-foot horizontal survey rake installed at vertical centerline in the IRT test section

C. Facility Instrumentation

Standard facility instrumentation includes the north and south bellmouth pitot-static rakes and an array of RTDs in D-corner. Facility total temperature measurements were acquired from a 24-probe array (4 rows of 6 RTD probes) mounted on the leading edge of the D-corner turning vanes. The north and south pitot-

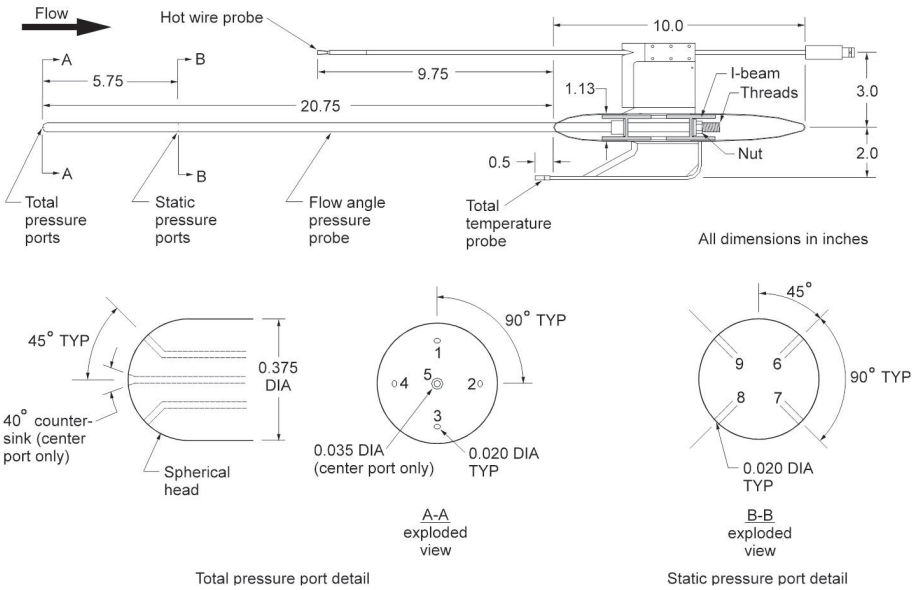

Figure 4. Hemispherical head probe total pressure ports. (A-A) total pressure port detail, (B-B) static pressure port detail.

static rakes measure total pressure and delta pressure, and are heated to prevent icing due to their position downstream of the spraybars.

D. Steady-State Data Acquisition System

Real time steady-state data acquisition and data display are provided by the NASA Glenn Escort Alpha System. This is the standard data acquisition and data display system used in the large test facilities at NASA Glenn. The system accommodates inputs from the Electronically Scanned Pressure (ESP) System, the facility distributed process control system, and any analog devices such as thermocouples, RTDs and pressure transducers. This system records all steady-state pressures and temperatures from the standard facility instrumentation and test specific hardware including the 9-ft survey rake and the 2D RTD array. It also records facility operational parameters such as spraybar air pressure and drive fan speed. An Escort program was specifically written to support the aero-thermal calibration in the IRT.

The ESP system used during the test program utilized thirty-two port rack mounted modules. For this test program ±5 psid modules were used. The accuracy in the pressure measurements made with the ESP System is 0.1 percent of full-scale of the module, or 0.005 psia for the ± 5 psid modules used.

E. Hot Wire Survey Rake and Instrumentation

A custom hot wire system has been developed for use at NASA GRC and is shown in Figure 5(a). The hot wire or film is connected to the TSI Incorporated (Shoreview, MN) IFA-100 Anemometer, Model 150 Transducer module. The output from the anemometer is fed into the National Instruments (NI) Corporation (Austin, TX) Data Acquisition (DAQ) System which is connected to a laptop with NI Labview software. A custom Labview program is written for the hot wire/film sensors which has the capability to accommodate up to 16 sensors across 4 PXI-6115 DAQ cards. A button trigger is connected between the hot wire data system and the facility steady-state data acquisition system, Escort, which enables both systems to be triggered simultaneously.

Turbulence intensity data were acquired with the hot wire/film survey rake shown in 5(b). The hot wire/film is installed so as to position the wire/film horizontally or along the Y-axis with respect to the test section. Prior to the construction of this rake the hot wires were mounted to the top of the 9-ft survey rake. Calibrations for the hot wires are performed in situ in the wind tunnel test section from minimum to maximum velocity at the beginning of testing for each position. Testing with the hot wire rake is only done in the incompressible regime, $M < 0.3$. Only single wires/films normal to the axial velocity are used as the calibration is conducted in situ.

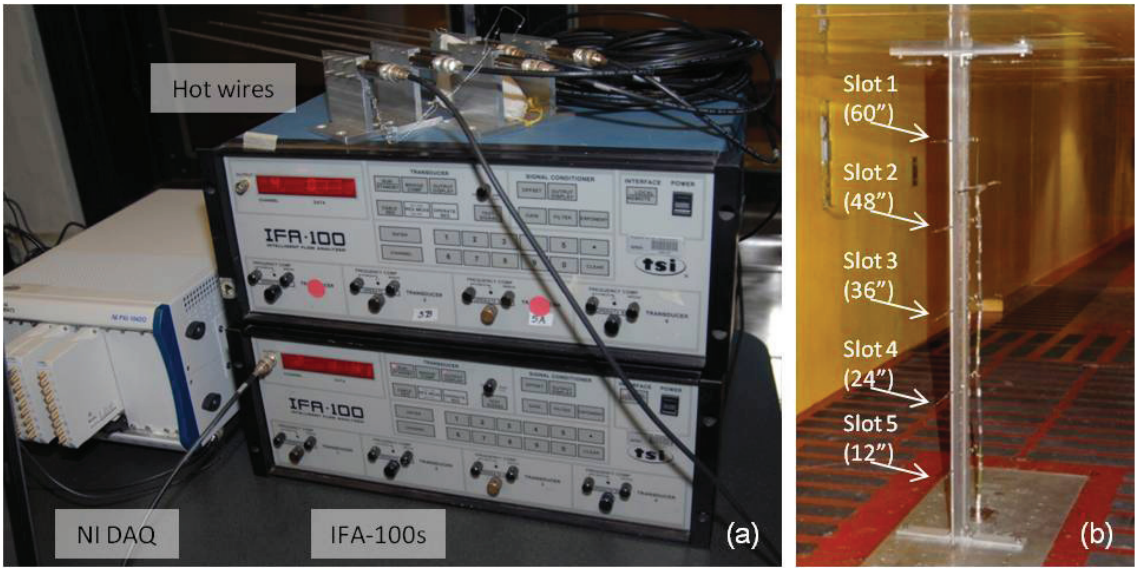

Figure 5. Hot wire/film anemometry system: (a) NI DAQ and IFA-100 (b) hot wire rake installed in the IRT test section with five hot wires and a pitot-static probe

IV. Test Matrix and Test Procedures

The IRT was operated with normal operational procedures during the aero-thermal calibration. Standard test procedure was to acquire two data readings for each test condition. Each reading was an average of 10 scans at a rate of 1 scan per second. For the 9-ft survey rake, and the hot wire survey rake, prior to taking a reading, the spatial standard deviation of the D-corner RTDs was verified to be within $\pm 0.5\,^{\circ}C$. During testing of the 2D RTD array, in addition to verifying the spatial standard deviation, the temporal standard deviation of the D-corner RTDs was verified to be within $\pm 0.1\,^{\circ}C$.

Table 1 illustrates the data points that were acquired with the 9-ft survey rake. During testing static temperature was held at $4.0\,^{\circ}C$[7].

Table 2 summarizes the data points that were recorded for the 2D RTD Array. During testing of the 2D RTD array, total temperature was set instead of static temperature. The operators were then instructed to go "hands off" of the temperature controls. To allow for a manageable total temperature swing of approximately $\pm 5.0\,^{\circ}C$, for each new sequence, total temperature was stabilized at the target temperature, i.e. $-10.0\,^{\circ}C$, at 220 knots prior to acquiring data. The data at the remaining velocities were acquired in the order of 50, 130, and 300 knots. Additionally, the spraybar air pressures were tested in the sequence of 0, 60, 30 psig. This was done so the spraybars would stabilize at their normal operating temperature of $80 - 85\,^{\circ}$ more quickly.

The hot wire survey rake test points are illustrated in Table 3. Turbulence data were collected at a tunnel total temperature of $7.8\,^{\circ}C$ to prevent the tunnel static temperature from dropping below freezing.

V. Data Reduction

U.S. customary units of measurement are used in the following data reduction. However, the icing community prefers a mixed set of units including airspeed in knots and temperature in degrees Celsius ($^{\circ}C$). Therefore, the details on the data reduction are presented as they are carried out in English units. The final results have been converted to and are presented in the units used by the icing community.

For the following calculations, the *bm* subscript refers to measured or calculated parameters associated with the two bellmouth pitot-static probes. The subscript *rake* refers to measured or calculated parameters associated with any of the probes on the 9-ft survey rake. Additionally, the subscript *local* refers to the measured or calculated corrected *rake* parameters which have been corrected by individual probe calibration coefficients and represent the true local properties in the test section. All of the local total pressures, static pressures, and Mach numbers are normalized by bellmouth parameters to arrive at recovery ratios. All of the equations utilized in the data reduction were compressible flow equations[8].

Table 1. Test matrix for the 9-ft survey rake.

Rake Position (horizontal)	Static temperature, $T_{T,ts}\,^{\circ}C$	Test Section Airspeed, $U_{ts} knots$	Spraybar air pressure, $P_{air}, psig$
CL	4.0	50,90,120,150,170,200,250	0,30,60
CL-6″	4.0	50,90,120,150,170,200,250	0,30,60
CL+6″	4.0	50,90,120,150,170,200,250	0,30,60
CL-12″	4.0	50,90,120,150,170,200,250	0,30,60
CL+12″	4.0	50,90,120,150,170,200,250	0,30,60
CL-18″	4.0	50,90,120,150,170,200,250	0,30,60
CL+18″	4.0	50,90,120,150,170,200,250	0,30,60
CL-24″	4.0	50,90,120,150,170,200,250	0,30,60
CL+24″	4.0	50,90,120,150,170,200,250	0,30,60

Table 2. Test matrix for the RTD Array.

Test Section total temperature, $T_{T,ts}\,^{\circ}C$	Test Section Airspeed, $U_{ts} knots$	Spraybar air pressure, $P_{air}, psig$
-30	50,130,220,300	0,30,60
-20	50,130,220,300	0,30,60
-10	50,130,220,300	0,30,60
-3	50,130,220,300	0,30,60
-2	50,130,220,300	0,30,60
-1	50,130,220,300	0,30,60
0	50,130,220,300	0,30,60
1	50,130,220,300	0,30,60
2	50,130,220,300	0,30,60
3	50,130,220,300	0,30,60
5	50,130,220,300	0,30,60

Table 3. Test matrix for the hot wire survey rake.

Rake Position (lateral)	Test Section total temperature, $T_{T,ts}\,^{\circ}C$	Test Section Airspeed, $U_{ts} knots$	Spraybar air pressure, $P_{air}, psig$
CL	7.8	50,90,120,150,170	0,30,60
CL-18″	7.8	50,90,120,150,170	0,30,60
CL-36″	7.8	50,90,120,150,170	0,30,60
CL+18″	7.8	50,90,120,150,170	0,30,60
CL+36″	7.8	50,90,120,150,170	0,30,60

A. Facility Calculations

The bellmouth pitot-static rakes in the IRT measure total pressure and delta pressure. Equation 1 shown below calculates the average that is taken of the bellmouth total pressure between the north and south pitot-static probes.

$$P_{T,bm} = \frac{(P_{T,north} + P_{T,south})}{2} \tag{1}$$

Static pressure was computed by the difference of total pressure from delta pressure. The north and south probes were calculated separately.

$$P_{S,north} = P_{T,north} - \Delta P_{north}, \qquad P_{S,south} = P_{T,south} - \Delta P_{south} \tag{2}$$

The static pressure of the bellmouth was then averaged using the static pressure readings from the north and south bellmouth pitot-static probes, equation 3.

$$P_{S,bm} = \frac{(P_{S,north} + P_{S,south})}{2} \tag{3}$$

Facility total temperature, equation 4, was calculated based on the average of the 24 RTDs on the leading edge of the D-corner turning vanes.

$$T_{T,davg} = \frac{1}{24}\sum_{i=1}^{24} T_{T,d,i} \tag{4}$$

Utilizing the bellmouth total pressure and static pressure, Mach number at the bellmouth is computed using equation 5.

$$M_{bm} = \sqrt{\frac{2}{\gamma - 1}\left[(\frac{P_{T,bm}}{P_{S,bm}})^{\frac{\gamma-1}{\gamma}} - 1\right]} \tag{5}$$

Facility dynamic pressure, equation 6 is then calculated using bellmouth Mach number, M_{bm} and bellmouth static pressure $P_{S,bm}$.

$$q_{bm} = \frac{\gamma}{2} P_{S,bm} \cdot M_{bm}^2 \tag{6}$$

B. 9-foot Survey Rake Calculations

Data collected by the 9-ft survey rake is used to construct Mach number and static pressure calibration curves. Additionally, the collected data is examined to check for flow quality in the facility.

The average of the four static pressure taps on each of the 11 probes was used to calculate the rake static pressure for each probe.

$$P_{S,rake} = \frac{(P_6 + P_7 + P_8 + P_9)}{4} \tag{7}$$

Mach number was computed based on the rake total pressure to static pressure ratio.

$$M_{rake} = \sqrt{\frac{2}{\gamma - 1}\left[(\frac{P_{T,rake}}{P_{S,rake}})^{\frac{\gamma-1}{\gamma}} - 1\right]} \tag{8}$$

The correction equations or local values for total and static pressure are based on the rake Mach number. C_o and C_q are functions of M_{rake} and are experimentally determined during calibration of the pressure probe flow angle[6]. Local static and total pressure are computed as shown.

$$P_{T,local} = P_{T,rake} - C_o(M_{rake})\left[P_{T,rake} - P_{S,rake}\right] \tag{9}$$

$$P_{S,local} = P_{T,local} - \frac{(P_{T,rake} - P_{S,rake})}{C_q(M_{rake})} \tag{10}$$

The local test section Mach number (equation 11) for each probe is determined using $P_{S,local}$ and $P_{T,local}$.

$$M_{local} = \sqrt{\frac{2}{\gamma - 1}\left[(\frac{P_{T,local}}{P_{S,local}})^{\frac{\gamma-1}{\gamma}} - 1\right]} \tag{11}$$

Local dynamic pressure in the test section is calculated per equation 12 below.

$$q_{local} = \frac{\gamma}{2} P_{S,local} \cdot M_{local}^2 \tag{12}$$

C. Flow Angularity

The following equations are used to calculate pitch and yaw flow angle data from the pressure data obtained from the 45 ° offset pressure ports on the front of the hemispherical head probe. The average of these four 45 ° offset pressure ports is used to calculate P_{avg}, equation 13.

$$P_{avg} = \frac{(P_1 + P_2 + P_3 + P_4)}{4} \tag{13}$$

The pressure coefficients C_α and C_β are calculated for both pitch and yaw. The pitch pressure coefficient, C_α, equation 14 is calculated using the 45 ° offset pressure ports in the pitch plane, P_1 and P_3 and the difference between the total pressure in the center of the hemispherical probe, P_5, and the average of all four 45 ° offset pressure ports. Similarly, the yaw pressure coefficient, C_β, equation 15 is calculated using the 45 ° offset pressure ports in the yaw plane, P_2 and P_4, and the difference between the total pressure in the center of the hemispherical probe, P_5, and the average of all four 45 ° offset pressure ports.

$$C_\alpha = \frac{(P_3 - P_1)}{(P_5 - P_{avg})} \tag{14}$$

$$C_\beta = \frac{(P_4 - P_2)}{(P_5 - P_{avg})} \tag{15}$$

Pitch angle, α, and yaw angle, β, are calculated using previously determined pitch and yaw pressure coefficients and M_{rake}.

$$\alpha = K_{0,\alpha}(M_{rake}) + K_{1,\alpha}(M_{rake})C_\alpha + \Delta_{\alpha,arm} + \Delta_{\alpha,level} \tag{16}$$

$$\beta = K_{0,\beta}(M_{rake}) + K_{2,\beta}(M_{rake})C_\beta + \Delta_{\beta,arm} + \Delta_{\beta,ruler} \tag{17}$$

The coefficients $K_{0,\alpha}$, $K_{1,\alpha}$, $K_{0,\beta}$, and $K_{2,\beta}$ were experimentally determined[6]. The delta coefficients are measurements made using a computer-aided inspection arm, an inclinometer, and a ruler.

D. Turbulence Intensity

During this particular test entry one hot wire and four hot film probes were used. The hot wire was positioned near the ceiling at 60-inches and the hot films were places in the remaining four slots below the hot wire. The hot wire and film probes were calibrated in situ in the IRT at the beginning of testing at each new position. In situ calibration data sweeps were completed at velocities of 50, 90, 120, 150, and 170 knots and with the spraybar air pressure at 0 psig. These in situ calibration data sweeps and a known velocity from a 5-hole hemispherical head probed attached to the side of the rake were used to develop coefficients A, B and n seen in King's Law[9] below, (equation 18).

$$E^2 = A + B \cdot Q^n \qquad or \qquad Q = \left[\frac{(E^2 - A)}{B}\right]^{1/n} \tag{18}$$

Once the coefficients were developed, King's Law was again used to calculate measured velocity from the hot wire/film voltages for each acquired data point. The variable Q is the measured velocity, and since single wires or films were used, it is assumed that Q equals the axial component only. Using the now calculated velocity values, a temporal mean velocity and standard deviation for each steady state data point, acquired at a rate of 1kHz for 10 seconds, is calculated. Dividing the root mean square of the instantaneous velocity by the mean velocity yields turbulence intensity.

E. 2D RTD Array Calculations

Total temperature data recorded by the 2D RTD array requires a flow recovery correction, equation 19. Experiments to determine the flow recovery coefficients for the RTDs on the 2D RTD array were performed in 2005[5].

$$T_{T,local} = (C_0 + C_1 M_{ts} + C_2 M_{ts}^2) T_{T,array} \tag{19}$$

This local total temperature is then used to develop a calibration curve between the 2D RTD array in the test section and the D-corner RTDs.

VI. Discussion of Results

Table 4 is a summary of Aero-Thermal flow quality goals for an icing wind tunnel[7]. The IRT flow quality meets or exceeds the goals for all of the parameters listed in Table 4. The data presented here is a representative set of results. A NASA contractor report will be published soon and will include all data acquired during the 2012 test.

Table 4. Aero-thermal flow quality goals for an icing tunnel test section.

Parameter	Measurement Uncertainty	Test Section Spatial Uniformity	Tunnel Centerline Temporal Stability
Airspeed	$\pm 1\%$	$\pm 2\%$	$\pm 2\%$
Static air temperature, -30 through $+5\,^{\circ}C$	$\pm 2\,^{\circ}C$	$\pm 1\,^{\circ}C$	$\pm 0.5\,^{\circ}C$
Flow Angularity	$\pm 0.25\,^{\circ}$	$\pm 2\,^{\circ}$	N/A
Turbulence ($P_{air} = 0 psig$)	$\pm 0.25\%$	$< 2\%$	$\pm 2\%$
Turbulence ($P_{air} = 60 psig$)	$\pm 0.25\%$	$< 2\%$	$\pm 2\%$

A representative set of results at 150 knots for Mach number is show in Figure 6. Mach number in the test section, M_{ts}, is normalized by Mach number at the bellmouth, M_{bm}, and plotted with respect to the width of the test section in inches, Figure 6. Delta Mach number, each major division on the vertical axis in Figure 6 helps to illustrate the absolute Mach number variation seen in the data. Also, examining Figure 6, it is seen that the spraybar air injection has a minimal affect on Mach number, increasing the variation in Figure 6(a) from 0.00345 to 0.0046 seen in Figures 6(b&c).

A representative set of results at 150 knots for total pressure is shown below in Figure 7. Total pressure in the test section, $P_{T,ts}$, is normalized by total pressure at the bellmouth, $P_{T,bm}$, and plotted with respect to the width of the test section in inches, Figure 7. A delta total pressure is seen in the bottom right corner of the plots to help relate the quantity of one tick in Figure 7 to the ratio presented. Additionally, examining Figure 7, it is seen that the spraybar air injection does have an affect on the total pressure distribution in the test section. The largest effects of the spray bars are seen at lower test section airspeeds and near the test section boundaries. For example in Figure 7 the effect of the spraybars is more pronounced at the inner wall (0-24 inches) and the outer wall (84-108 inches). The flow in the core of the test section is minimally affected.

A representative set of results at 150 knots for static pressure is shown in Figure 8. Static pressure in the test section, $P_{S,ts}$, is normalized by static pressure at the bellmouth, $P_{S,bm}$, and plotted with respect to the width of the test section in inches, Figure 8. A delta static pressure is shown in the bottom right corner of the plots to help relate the quantity of one tick in Figure 8 to the ratio presented. Also, examining Figure 8 further, it is seen that the spraybar air injection does not have a significant effect on the static pressure distribution in the test section.

A representative set of results at 130 knots for total temperature is shown in Figure 9. Test section total temperature, $T_{T,ts,array}$,$^{\circ}\,C$, is shown plotted with respect to the width of the test section in inches, Figure 9. At a total temperature test point of $-1°C$ the test section temperature variation is no more than $\pm 0.25°C$. However, at colder total temperature test points of $-30°C$ the test section variation is approximately $\pm 0.5°C$. This larger variation is seen because the $80 - 85°C$ spraybar air is more pronounced in the test section at the much colder temperatures near the bottom of the IRT operating range.

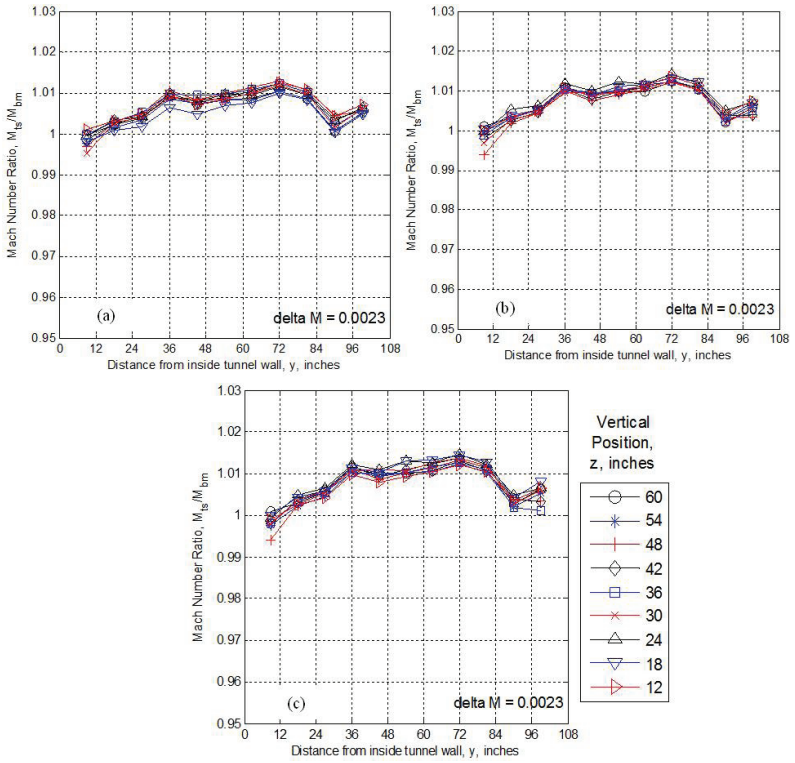

Figure 6. Mach number distribution data from the IRT test section. Data collected using the 9-ft survey rake mounted at 9 vertical positions over several tunnel runs. The test section Mach number data was normalized using the bellmouth Mach number measurement. Approximate Mach number delta is indicated for each test section setting. (a) $U_{ts} = 150knots$**,** $P_{air} = 0psig$**. (b)** $U_{ts} = 150knots$**,** $P_{air} = 30psig$**. (c)** $U_{ts} = 150knots$**,** $P_{air} = 60psig$**.**

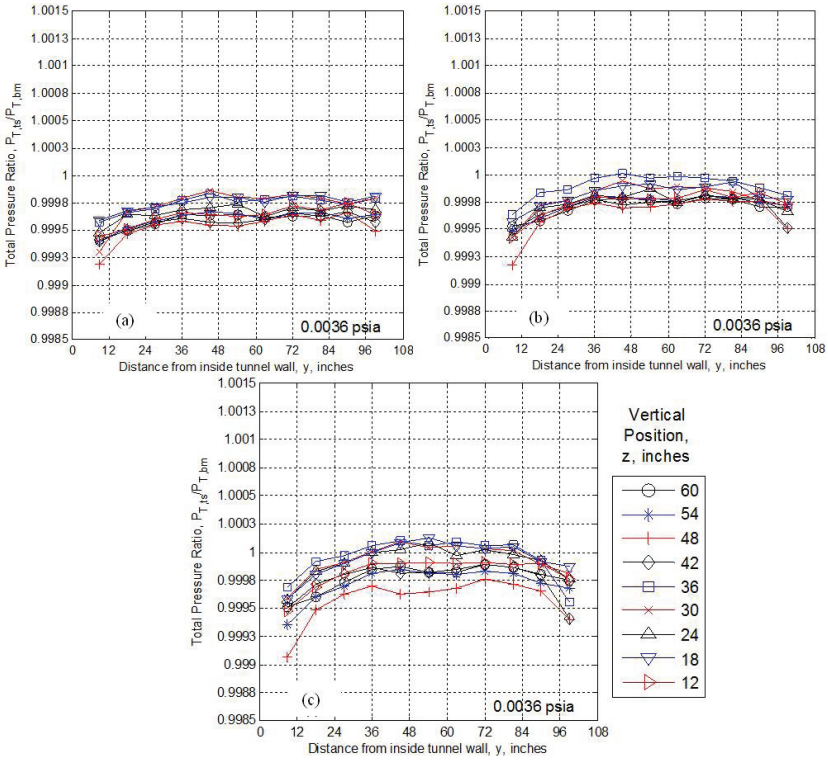

Figure 7. Total pressure distribution data from the IRT test section. Data collected using the 9-ft survey rake mounted at 9 vertical positions over several tunnel runs. the test section total pressure data is normalized using the bellmouth total pressure measurement. (a) $U_{ts} = 150knots$**,** $P_{air} = 0psig$**. (b)** $U_{ts} = 150knots$**,** $P_{air} = 30psig$**. (c)** $U_{ts} = 150knots$**,** $P_{air} = 60psig$**.**

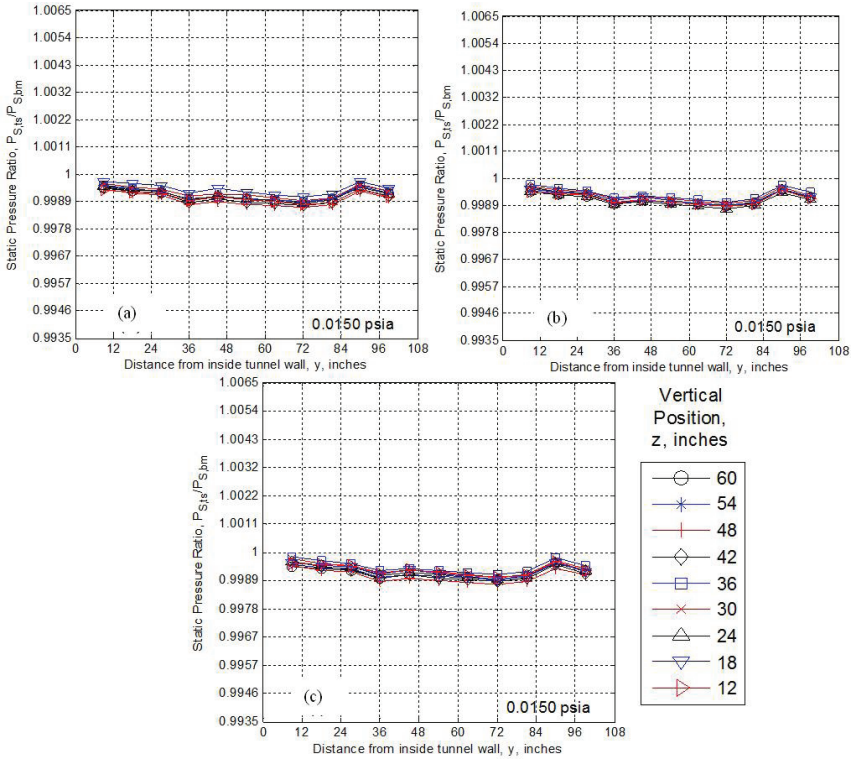

Figure 8. Static pressure distribution data from the IRT test section. Data collected using the 9-ft survey rake mounted at 9 vertical positions over several tunnel runs. (a) $U_{ts} = 150knots$, $P_{air} = 0psig$. **(b)** $U_{ts} = 150knots$, $P_{air} = 30psig$. **(c)** $U_{ts} = 150knots$, $P_{air} = 60psig$.

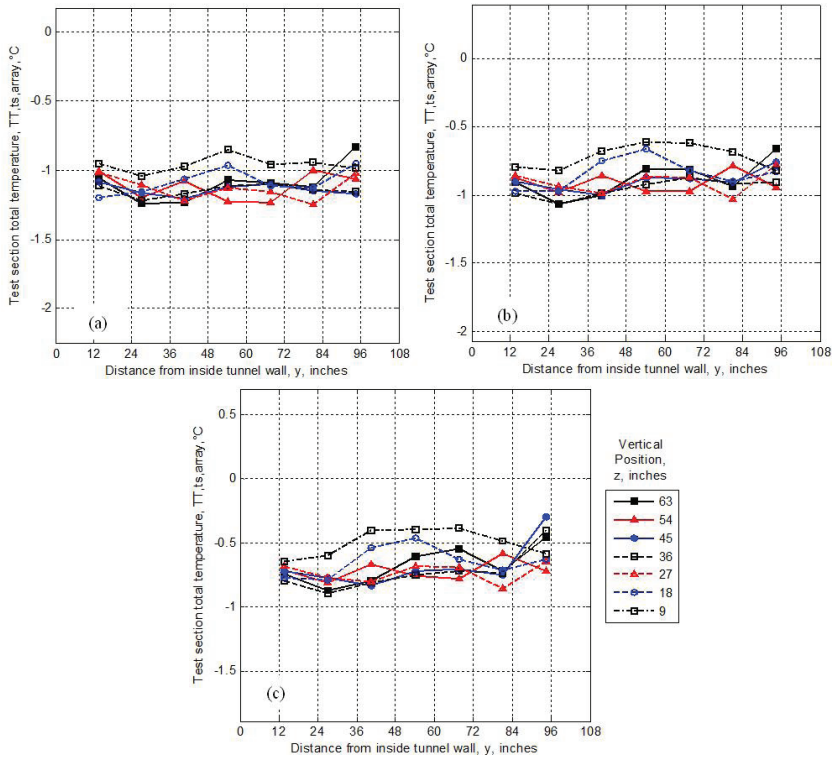

Figure 9. Total temperature data from the IRT test section at D-corner total temperature of $-1\,^{\circ}C$. **Data collected using the 2D RTD array. (a)** $U_{ts} = 130knots$, $P_{air} = 0psig$. **(b)** $U_{ts} = 130knots$, $P_{air} = 30psig$. **(c)** $U_{ts} = 130knots$, $P_{air} = 60psig$.

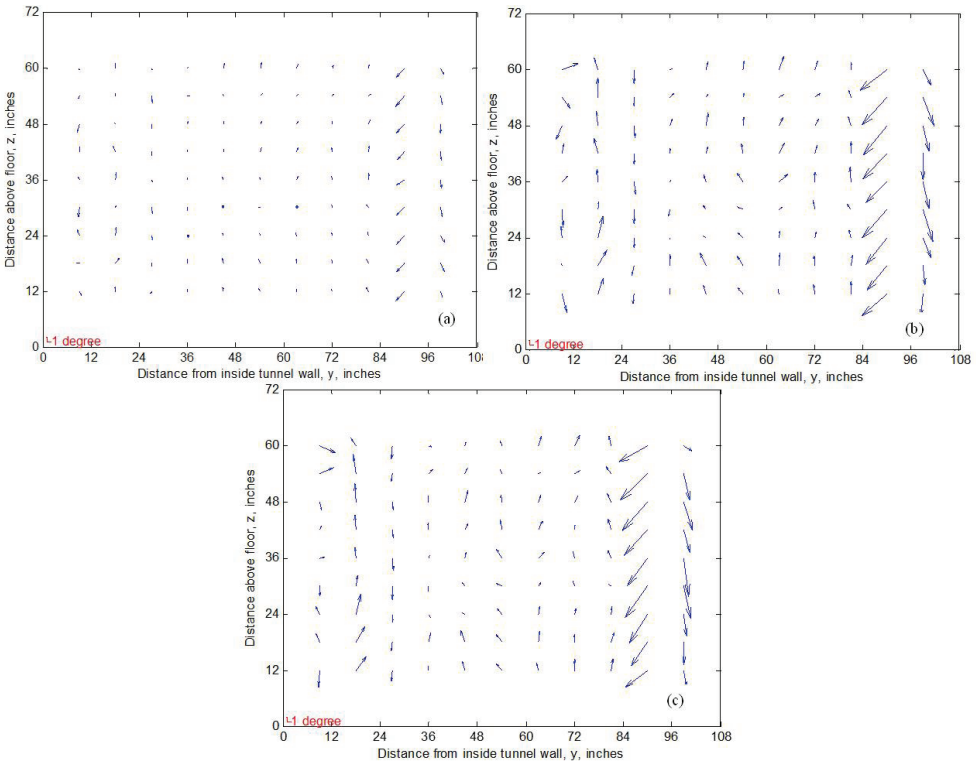

Figure 10. Flow angularity data in the IRT from the 9-ft survey rake mounted in the 9 vertical positions completed during testing. (a) $U_{ts} = 150knots$**,** $P_{air} = 0psig$**. (b)** $U_{ts} = 150knots$**,** $P_{air} = 30psig$**. (c)** $U_{ts} = 150knots$**,** $P_{air} = 60psig$**.**

A representative set of results at 150 knots for the test section flow angularity as measured by the 5-hole probes mounted on the 9-ft survey rake is shown in Figure 10. The vectors shown in Figure 10 only reflect the magnitude and direction of the local air flow, but not airspeed. For reference, $+1°$ in pitch and yaw is noted on each figure. Overall, the flow angularity in the IRT test section is acceptable for an icing facility. The wall flow angularity behaviour has been seen in previous data sets as far back as 2004. Most of the variation in the flow angle orientation is probably due to disturbances generated by the spraybars

Data shown in Figure 11 illustrates the turbulence intensity seen at the horizontal and vertical centerline of the test section with a spraybar air pressure of 0 psig. Turbulence intensity, u'/U, is shown plotted with respect to test section velocity, $U(kts)$, Figure 11. Facility changes that could affect turbulence intensity are summarized in the bottom right of Figure 11. The standard deviations shown on the 2009 and 2012 data are from 4 time traces taken at the same condition. The data is not available to develop standard deviations for data from 2005 and before.

A representative set of results at 150 knots for turbulence intensity is shown in Figure 12. The turbulence intensity, u'/U, is plotted with respect to the turn table centerline survey plane. A higher turbulence at centerline is typically seen due to the spray bar center support. Another contributing factor which is new this calibration cycle, is 7 air-only atomizing nozzles located at the bottom center of the spraybars. These were added to get the icing cloud to mix appropriately. The IRT will not have the low-turbulence levels of a wind tunnel used for aerodynamics testing due to the lack of flow manipulators like screens and honeycomb straighteners due to the influence of the sparybars. The turbulence intensity has been found to be 2% or less.

As mentioned, one of the primary goals of this calibration cycle was to update the aero-thermal calibration curves used in the computing subroutine IRTAT which is used to set conditions in the test section. Figure 13, Figure 14, and Figure 15 are the updated calibration relationships for Mach number, static pressure, and total temperature. It can been seen that the curves are linear in nature which is what is most desirable for calibration relationships.

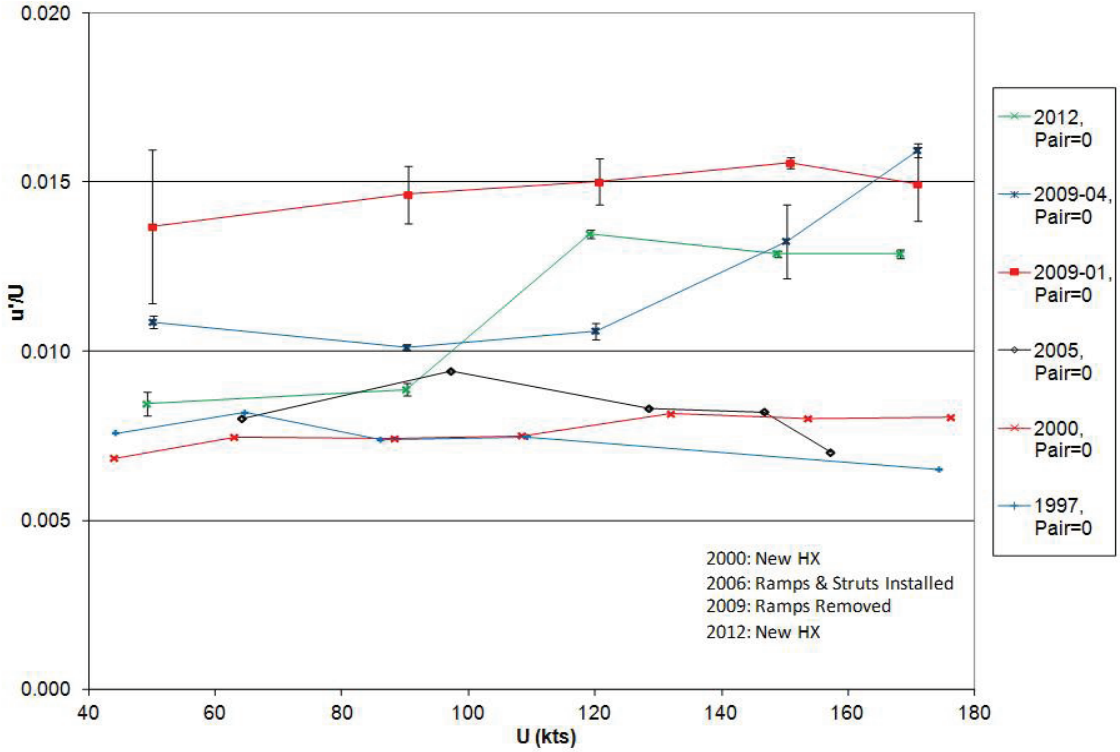

Figure 11. IRT Turbulence Intensity, Historical Comparison @ CL/CL, $P_{air} = 0psig$.

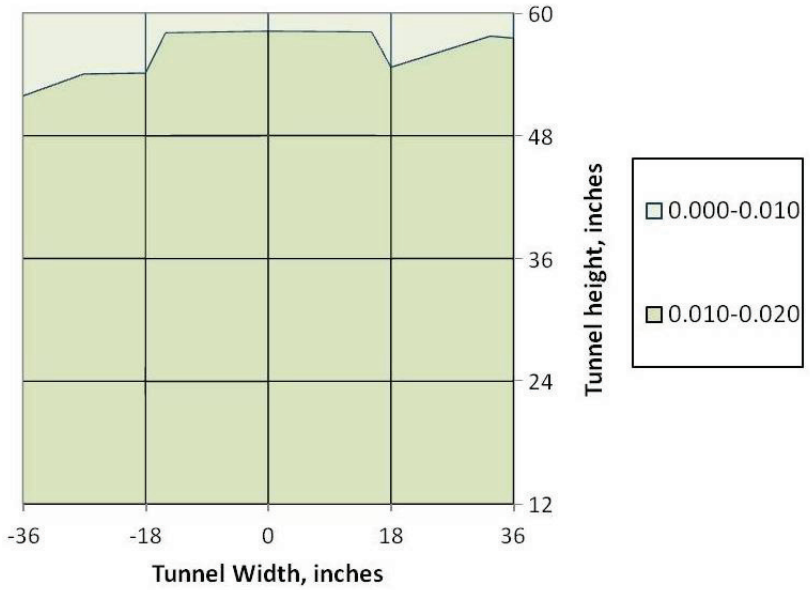

Figure 12. Turbulence Intensity Uniformity, u'/U **,from the hot wire rake.** $U_{ts} = 150knots$, $P_{air} = 0psig$.

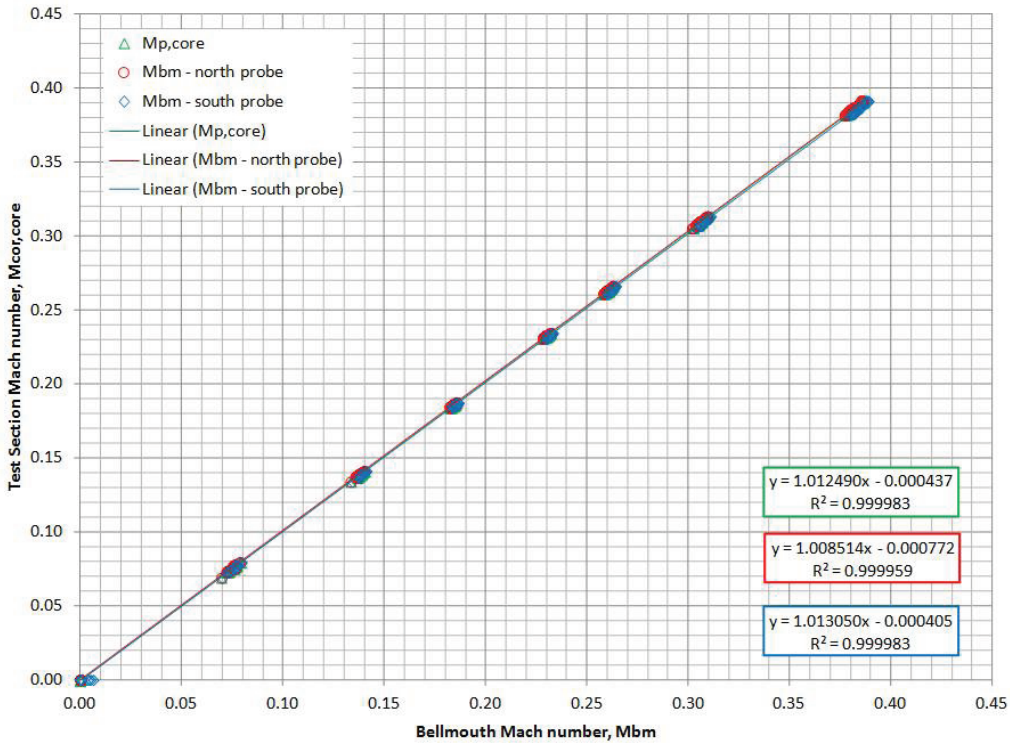

Figure 13. Mach number calibration for the IRT from the 2012 full aero-thermal calibration.

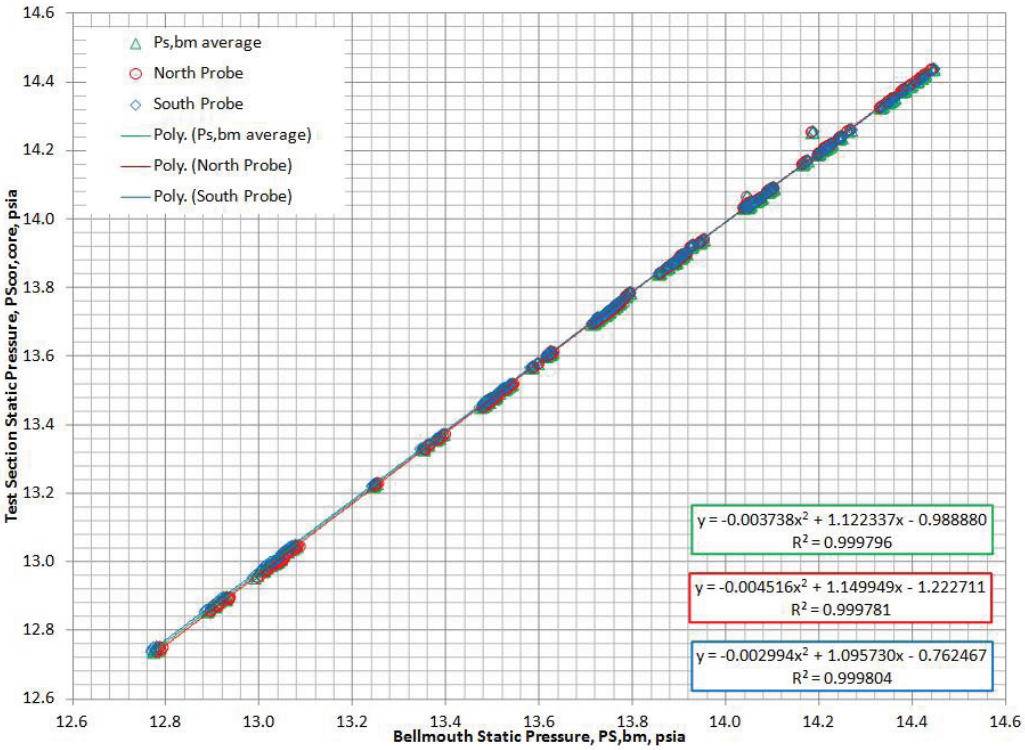

Figure 14. Static pressure calibration for the IRT from the 2012 full aero-thermal calibration.

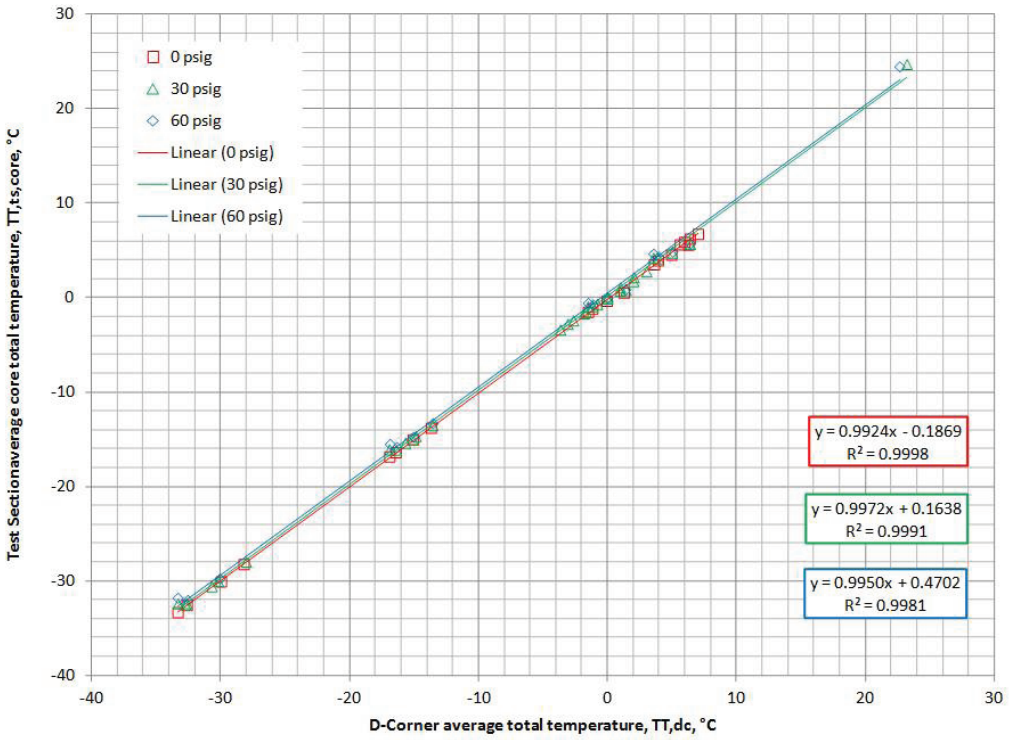

Figure 15. Total temperature calibration for the IRT from the 2012 full aero-thermal calibration.

VII. Summary and Conclusions

The data acquired during the 2012 calibration entry shows that the pressures are consistent with previous calibrations and there has been an improvement on the spatial temperature deviation of the heat exchanger. The temperature profile in the IRT was found to be much more uniform with the new heat exchanger than it was with the previous heat exchanger. The turbulence intensity has been found to be 2% or less. Test section spatial uniformity and tunnel centerline temporal stability meet the aero-thermal flow quality goals listed in Table 4. A new set of calibration curves have been developed and implemented for static pressure, Mach number, and total temperature.

Acknowledgements

I would like to recognize Laura E. Steen for the time she dedicated to the aero-thermal calibration testing during January 2012 and the time she provided to review this paper. Also, many thanks go out to the hard working engineering and technician staff at the IRT without whom none of this testing would be possible.

References

[1]Van Zante, J. F., Ide, R. F., and Steen, L. E., "NASA Glenn Icing Research Tunnel: 2011 Cloud Calibration Procedure and Results," *Atmospheric and Space Environments Conference*.

[2]Steen, L. E., Van Zante, J. F., Broeren, A. P., and Kubiak, M. J., "NASA Glenn Icing Research Tunnel: Flow Quality Surveys in the Settling Chamber of the NASA Glenn Icing Research Tunnel (2011 Tests," *4th AIAA Atmospheric and Space Environments Conference*, New Orleans(submitted for publication), June 2012.

[3]Clark, K., Malinowski, M., Loth, E., Steen, L. E., Van Zante, J. F., and Ide, R. F., "Air Flow and Liquid Water Concentration Simulations of the 2012 NASA Glenn Icing Research Tunnel," *Atmospheric and Space Environments Conference*, AIAA, New Orleans(submitted for publication), June 2012.

[4]Soeder, R.H., Sheldon, D.W., Ide, R.F., Spera, D.A. and Andracchio, C.R., "NASA Glenn Icing Research Tunnel User Manual'," NASA/TM-2003-212004, 2003.

[5]Gonsalez, J. and Arrington, E., "Improvements to the Total Temperature Calibration of the NASA Glenn Icing Research Tunnel," NASA/CR-2005-213875, AIAA-2005-4276, 2005.

[6]Gonsalez, J. and Arrington, E., "Five-Hole Flow Angle Probe Calibration for the NASA Glenn Icing Research Tunnel," 2001.

[7]"Calibration and Acceptance of Icing Wind Tunnels,", SAE Standards ARP(Aerospace Recommended Practice)5905, 2003.

[8]Staff, A. R., "Equations, Tables, and Charts for Compressible Flow," Report 1135, National Advisory Committee for Aeronautics, 1953.

[9]Tropea, C., Yarin, A. L., and Foss, J. F., editors, *Springer Handbook of Experimental Fluid Mechanics*, Springer, 2007.